Meteoritics & Planetary Science 43, Nr 4, 657–674 (2008)
Abstract available online at http://meteoritics.org

Evolution of the winonaite parent body: Clues from silicate mineral trace element distributions

Christine FLOSS[1, 2*], Ghislaine CROZAZ[1, 3], Brad JOLLIFF[3], Gretchen BENEDIX[4], and Shannon COLTON[5]

[1]Laboratory for Space Sciences, [2]Physics Department, [3]Department of Earth and Planetary Sciences,
Washington University, One Brookings Drive, Saint Louis, Missouri 63130, USA
[4]Department of Mineralogy, The Natural History Museum, Cromwell Road, London, SW7 5BD, United Kingdom
[5]Southwest Research Institute, San Antonio, Texas 78238, USA
[*]Corresponding author. E-mail: floss@wustl.edu

(Received 14 May 2007; revision accepted 27 September 2007)

Abstract–We have measured the trace element compositions of individual plagioclase, pyroxene, and olivine grains in 6 different winonaites that span the range of textures and mineralogies observed in these meteorites. Textural evidence in these meteorites, including the presence of a plagioclase/clinopyroxene-rich lithology and coarse-grained olivine lithologies, suggests that they may have experienced some silicate partial melting. However, trace element distributions in these lithologies do not show any clear signatures for such an event. Pyroxene trace element compositions do exhibit systematic trends, with abundances generally lowest in Pontlyfni and highest in Winona. The fact that the same trends are present for both incompatible and compatible trace elements suggests, however, that the systematics are more likely the result of equilibration of minerals with initially heterogeneous and distinct compositions, rather than partial melting of a compositionally homogeneous precursor. The winonaites have experienced brecciation and mixing of lithologies, followed by varying degrees of thermal metamorphism on their parent body. These factors probably account for the variable bulk rare earth element (REE) patterns noted for these meteorites and may have led to re-equilibration of trace elements in different lithologies.

INTRODUCTION

Primitive achondrites have, in the last decade, been recognized as a distinct class of meteorites intermediate between chondrites and achondrites. They typically exhibit achondritic textures, but have retained at least some primitive compositional features. A wide variety of meteorites have been called primitive achondrites, but the most well-defined groups include the acapulcoites and lodranites, and the winonaites and related silicate inclusions in IAB iron meteorites. Primitive achondrites derive their importance from the fact that they have experienced only limited melting often accompanied by metamorphism. They, therefore, provide valuable insights into early differentiation processes on asteroids.

The winonaites are a relatively small group (about a dozen known members) of primitive achondrites that have essentially chondritic mineralogies and bulk chemical compositions. They have oxygen isotopic compositions similar to IAB iron meteorites (Clayton and Mayeda 1996) and are petrographically similar to angular silicate inclusions in these meteorites, suggesting the formation of both groups of meteorites on a common parent body (e.g., Benedix et al. 2000). Comprehensive petrologic studies of winonaites have been published (Kimura et al. 1992; Benedix et al. 1998; Yugami et al. 1998, 1999), but there is no consensus as to how these objects formed. Nevertheless, it is clear that the winonaites have experienced extensive thermal metamorphism, resulting in equigranular textures in most samples, and at least limited partial melting, as is evident from the presence of Fe,Ni metal and troilite veins. The winonaites have also experienced brecciation, resulting in the juxtaposition of lithologies with distinctly different grain sizes and mineralogies. Some of these lithologies may be the result of silicate partial melting (e.g., Benedix et al. 1998).

The IAB iron meteorites have been more extensively studied than the winonaites, and a variety of theories have been proposed for their origin. These include solid-state growth in the solar nebula (Wasson 1970); crystallization from impact melt pools in a chondritic megaregolith (Wasson et al. 1980; Choi et al. 1995; Wasson and Kallemeyn 2002); and melting on a partially differentiated asteroid (Kracher 1982, 1985; Takeda et al. 2000). Benedix et al.

(2000) proposed a hybrid model for the formation of the winonaites and IAB irons that combined features from several previous models. They argued that the 2 meteorite groups formed on a common parent body that underwent partial melting and incomplete differentiation. This was followed by catastrophic impact breakup and reassembly of the debris, allowing molten metal from the interior of the parent body to mix with near-surface silicate material. Slow cooling of the re-accreted body resulted in a period of extended metamorphism.

We are systematically studying the trace element distributions within these meteorites in order to better understand the evolution of their parent body. In particular, we are interested in evaluating the roles that silicate partial melting and metamorphism may have played. Trace element abundances have been measured in bulk samples, but the data are difficult to interpret because of the heterogeneous distribution of major and minor minerals that exists even on a thin section scale. Chondrite-normalized rare earth element (REE) patterns in both winonaites and IAB silicate inclusions range from almost flat to V-shaped, with low absolute REE abundances and positive Eu anomalies, to higher REE abundances and striking negative Eu anomalies (e.g., Davis et al. 1977; Prinz et al. 1980; Yamamoto et al. 1991; Kimura et al. 1992; Kallemeyn 1997). It has been suggested that much of this variability is likely due to the incomplete sampling of phosphates (Kallemeyn and Wasson 1985), which are major REE carriers in these meteorites. We are avoiding such heterogeneity problems by making in situ measurements of individual minerals in the samples.

We report here results from 6 winonaites that cover the range of textural and mineralogical variations observed in these meteorites. Preliminary results were reported by Floss et al. (2003, 2006).

EXPERIMENTAL

We obtained one thin section of each of the 6 winonaites investigated here. Winona (USNM 854-1), Mount Morris, Wisconsin (USNM 1198-2), Pontlyfni (USNM 6904) and Tierra Blanca (USNM 6154-1) are from the Smithsonian Institution, Hammadah al Hamra (HaH) 193 was provided by A. Bischoff of the University of Münster, and Northwest Africa (NWA) 1463 was provided by A. Rubin from UCLA. Samples were initially documented using a JEOL 840a scanning electron microprobe (SEM) operated at 10 kV and 5 nA beam current. Each of the sections was mapped in a tiled pattern of slightly overlapping areas, which were collected at 50× magnification (100× for Pontlyfni) in 1024^2 pixels for backscattered electrons (BSE) and 256^2 pixels for X-ray elemental signals of Na, Mg, Al, Si, P, S, Ca, Cr, Ti, and Fe, resulting in a spatial resolution of ~7 μm/pixel for the elemental distribution images. The elemental maps were then processed using custom software to identify individual mineral phases and to determine the modal compositions of the samples. Details of this software processing routine are given in Floss et al. (2007).

Concentrations of the REE and other trace elements were determined using the modified Cameca IMS 3f ion microprobe at Washington University, according to techniques described by Zinner and Crozaz (1986a). All analyses were made using an O^- primary beam and energy filtering at low mass resolution to remove complex molecular interferences. The resulting mass spectrum is deconvolved in the mass ranges K-Ca-Sc-Ti, Rb-Sr-Y-Zr, and Ba-REE to remove simple molecular interferences that are not eliminated with energy filtering (Alexander 1994; Hsu 1995). Sensitivity factors for the REE in pyroxene and Ca-phosphate are from Zinner and Crozaz (1986b) and for plagioclase are from Floss and Jolliff (1998). Sensitivity factors for other elements in the silicates are from Hsu (1995) and are listed in Table 1 of Floss et al. (1998). Absolute concentrations are determined using sensitivity factors relative to Si for the silicates and Ca for the phosphates. The CaO concentrations used for the phosphates (apatite and merrillite) were determined from EDX analyses of representative grains from each meteorite, whereas SiO_2 concentrations for the silicates are averages of values determined by electron microprobe. SiO_2 concentrations for silicates from Tierra Blanca are the average values listed in King et al. (1981). Four measurements in a fine-grained lithology from Pontlyfni correspond to a mixture of minerals; for these analyses, we averaged the SiO_2 concentrations of all the minerals involved (plagioclase, orthopyroxene, clinopyroxene, and olivine) and used this value for determining REE concentrations. Although this introduces some uncertainty in the absolute REE concentrations of the analysis areas, this is limited to ±15% relative and does not affect any of the conclusions based on these analyses. REE abundances in the figures are normalized to the CI abundances of Anders and Grevesse (1989).

SAMPLE DESCRIPTIONS

The winonaites studied here exhibit a range of petrographic features that reflect the varying degrees of thermal metamorphism they have experienced. In addition, some winonaites contain unusual lithologies that may be related to silicate partial melting on the parent body (e.g., Benedix et al. 1998). Figure 1 shows the range in textures observed in the winonaites and Fig. 2 documents particular lithologies seen in these samples. Modal abundances are listed in Table 1. Each meteorite is discussed in detail below, in approximate order of increasing degree of equilibration.

NWA 1463

NWA 1463 was classified as a winonaite based on its mineralogy and oxygen isotopic composition (Benedix et al. 2003). Like most winonaites, it is dominated by sub-equal amounts of orthopyroxene and metal and sulfides, with lesser

Table 1. Modal abundances (vol%) of minerals in winonaites[a].

	NWA 1463	Pontlyfni	Winona	Mt. Morris	Tierra Blanca	HaH 193
Orthopyroxene	46.4	29.9 (26.6)[b]	53.1	47.5	39.3	48.0
Clinopyroxene	7.7	3.6 (4.4)	0.6	2.9	3.0	0.7
Amphibole						4.1
Olivine	8.6	20.8 (20.5)	14.6	16.2	16.5	9.7
Plagioclase	6.5	10.5 (12.5)	11.4	6.8	7.7	10.9
Phosphate	0.7	Trace	0.4	0.1	Trace	0.1
Opaque minerals[c]	30.6	35.1 (36.0)	20.0	26.5	33.6	26.7

[a]Modified from Floss et al. (2007).
[b]Values in parentheses include fine-grained, plagioclase/clinopyroxene-rich lithology.
[c]Includes Fe,Ni metal, FeS, chromite, schreibersite, phosphide, and weathering products.

amounts of olivine, plagioclase, and clinopyroxene (Table 1). However, unlike winonaites with equigranular textures and numerous triple junctions among equant mineral grains, NWA 1463 contains abundant relict chondrules set in a recrystallized groundmass, and texturally resembles a type 5 chondrite (Fig. 1a). It also lacks the Fe,Ni metal and FeS veins common in other winonaites that are indicative of partial melting. Based on these features, Benedix et al. (2003) suggested that NWA 1463 may be the most primitive of winonaites and, therefore, could most closely resemble the precursor material from which these meteorites originated.

However, Benedix et al. (2006) noted that chromite compositions in NWA 1463 fall significantly outside of the range of winonaite chromites and that it does not appear to contain graphite, which is commonly observed in winonaites. Moreover, it may also be paired with NWA 725, which is classified as an acapulcoite. The oxygen isotopic compositions of both meteorites are similar and extend to lower $\delta^{18}O$ values than most winonaites, but do not fall within the range of acapulcoite and lodranite oxygen isotopic compositions. Trace element data for these meteorites also show a number of similarities, but several important differences as well (unpublished data from our laboratory). Thus, it is not immediately clear if these 2 meteorites are indeed paired and whether or not they should in fact be classified as winonaites. Here we report trace element data for NWA 1463 and consider it within the context of other winonaites, but it should be kept in mind that the classification of this meteorite remains somewhat uncertain.

Pontlyfni

Pontlyfni is the only member of this group that is an observed fall (1931). It is one of the most fine-grained winonaites, with an average grain size of ~75 μm (Benedix et al. 1998). Like NWA 1463, it contains sub-equal amounts of orthopyroxene and metal and sulfides, the latter occurring as large veins throughout the sample. Clinopyroxene and plagioclase are minor phases, but olivine is a factor of 2 more abundant in Pontlyfni than in NWA 1463 (Table 1). Pontlyfni also contains discrete areas that are highly enriched in plagioclase and clinopyroxene, which were initially described by Benedix et al. (1998). These regions are significantly more fine-grained than the matrix (Fig. 2a) with equigranular textures, and have irregular borders with the surrounding matrix. Benedix et al. (1998) cited the presence of this lithology as evidence for silicate partial melting on the winonaite parent body, as the mineral associations are those expected from crystallization of a basaltic partial melt.

Winona

Winona, the namesake of this group of meteorites, has an equigranular texture that is more coarse-grained than that of Pontlyfni (Fig. 1b), with an average matrix grain size of ~100 mm (Benedix et al. 1998). It is dominated by orthopyroxene, with roughly equal amounts of olivine, plagioclase, metal, and sulfides (Table 1), and contains only trace amounts of clinopyroxene and phosphate. Like Pontlyfni, the metal and sulfides are present as veins throughout the section. In addition, Winona contains regions that are significantly more coarse-grained than the rest of the meteorite (300–500 μm average grain size) and that consist predominantly of olivine grains (Fig. 2b). Benedix et al. (1998) interpreted these olivine-rich domains as partial melt residues, from elsewhere on the winonaite parent body, that were incorporated into the current sample by impact mixing. They estimated that such residues implied as much as 45% partial melting of a chondritic precursor.

Mount Morris

Mount Morris is similar to Winona, both texturally and modally, consisting predominantly of medium-grained (~125 μm) equigranular orthopyroxene and olivine, with lesser amounts of plagioclase and clinopyroxene. Metal and sulfide veins are present, as are regions that are significantly more coarse-grained than the matrix. However, unlike Winona, the coarse regions in our section of Mount Morris do not exhibit a different silicate mineralogy from the more fine-grained matrix areas, an observation also made by Benedix et al. (1998).

Tierra Blanca

Tierra Blanca is one of the most coarse-grained winonaites with an equigranular texture (Fig. 1c). It has an average grain size of ~190 μm with abundant triple junctions, indicating

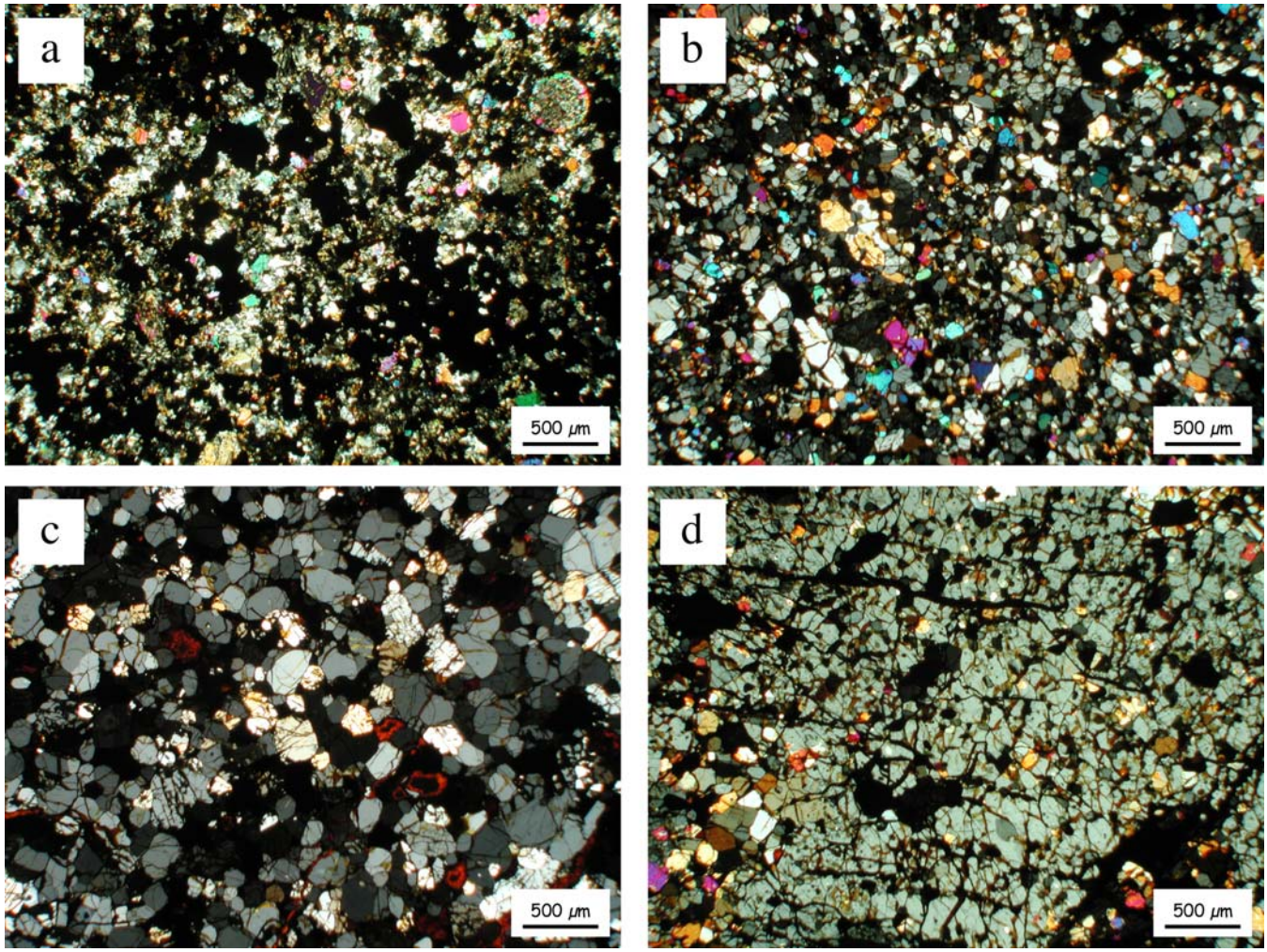

Fig. 1. Transmitted light (cross polarized) photomicrographs of winonaite textures: a) NWA 1463 resembles a type 5 chondrite, with relict chondrules (e.g., upper right) in a recrystallized matrix; b) Winona has a medium-grained equigranular texture, but also contains regions that are considerably more coarse-grained than the area shown; c) Tierra Blanca is one of the more coarse-grained winonaites and also contains large, poikilitic, calcic pyroxenes; d) HaH 193 consists of very large optically continuous orthopyroxene grains that enclose smaller grains of olivine and plagioclase.

extensive recrystallization (Benedix et al. 1998). Like other winonaites, it consists of sub-equal amounts of orthopyroxene and metal and sulfides (most of which have been altered by terrestrial weathering). It also contains large calcic pyroxene grains, which poikilitically enclose smaller grains of olivine, plagioclase and orthopyroxene (Fig. 2c). These grains can reach up to 9 mm in size (King et al. 1981; Benedix et al. 1998) and most likely formed through solid-state metamorphism (e.g., de Wit and Strong 1975; Kretz 1994). Also present in Tierra Blanca are coarse-grained clumps of olivine, similar to those observed in Winona.

HaH 193

Hammadah al Hamra 193 is unique among the winonaites (Floss et al. 2007). Instead of having a granoblastic texture, this winonaite consists of very large (up to 5 mm), optically continuous orthopyroxene grains (Fig. 1d) that enclose smaller grains of olivine and plagioclase. Interstitial to the orthopyroxene poikiloblasts are clumps of coarse equigranular olivine grains similar to those observed in Winona and other winonaites, and large (up to 2 mm) grains of amphibole that are associated with and locally enclose smaller grains of olivine, plagioclase, and clinopyroxene (Fig. 2d). Floss et al. (2007) identified the amphibole as fluoro-edenite and argued that it formed in the solid state through the replacement of clinopyroxene, probably in a reaction between clinopyroxene and plagioclase. Although our section of HaH 193 has a relatively low modal abundance of olivine (Table 1), similar to that noted in NWA 1463, another section of this meteorite examined by Floss et al. (2007) has higher olivine abundances, like those of the other winonaites studied here.

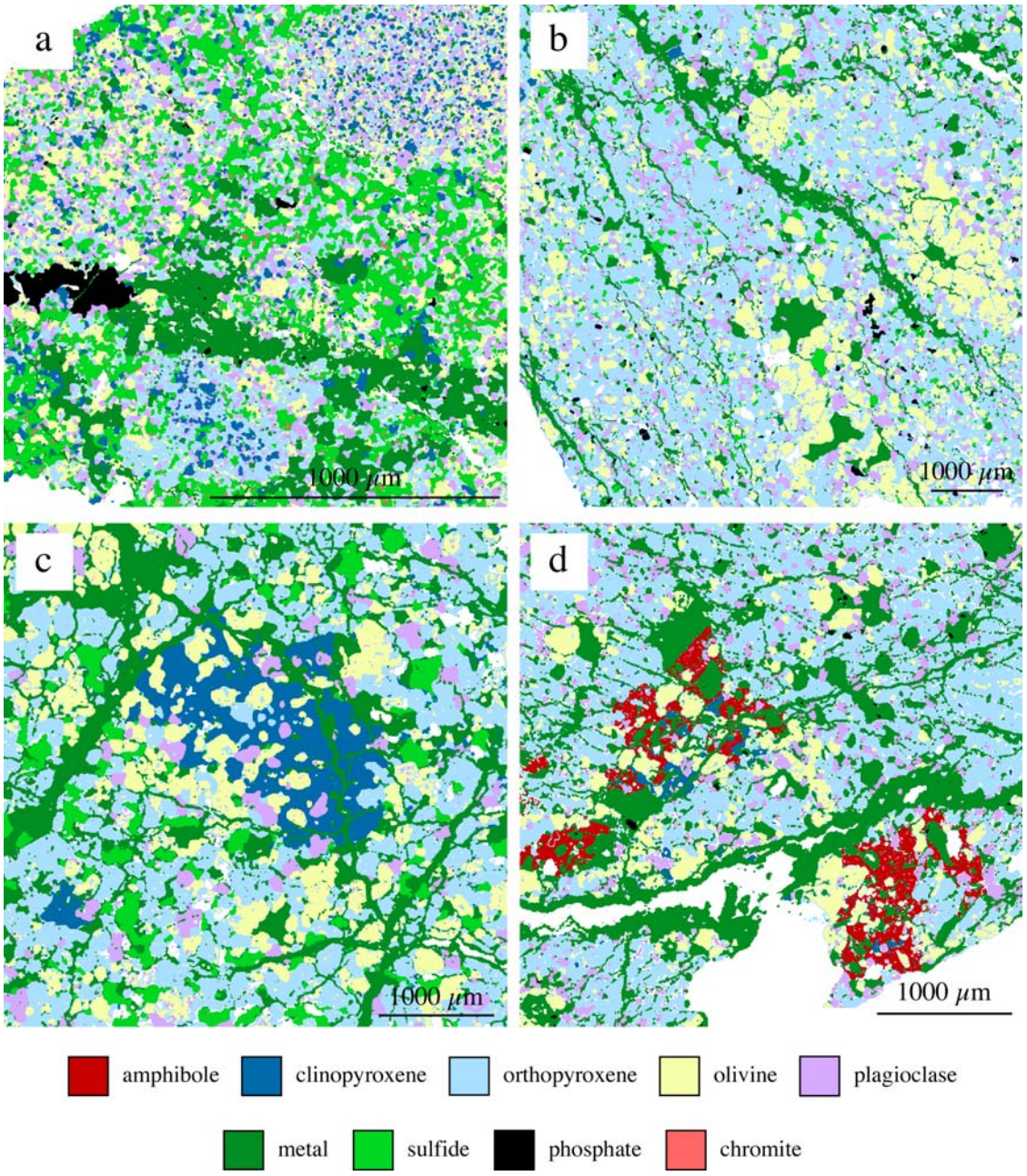

Fig. 2. Elemental composite maps of different lithologies in winonaites: a) fine-grained, plagioclase/clinopyroxene-rich areas within the matrix of Pontlyfni; b) coarse-grained olivine-rich regions in Winona; c) large clinopyroxene grain in Tierra Blanca poikilitically enclosing smaller grains of olivine and plagioclase; and d) poikilitic grains of amphibole (fluoro-edenite) in HaH 193.

RESULTS

We obtained minor and trace element data for plagioclase, clinopyroxene, orthopyroxene, and olivine from all 6 winonaites studied; these data are summarized in Table 2. In addition, REE abundances were determined in phosphate grains from the 4 winonaites with grains large enough to measure in the ion microprobe (~20 μm); these data are shown in Table 3.

Plagioclase

Chondrite-normalized REE patterns for plagioclase are LREE-enriched with large positive Eu anomalies (Fig. 3a); REE heavier than Gd are below detection limits in plagioclase grains from all the meteorites studied (Table 2a). Abundances are relatively uniform in most of the winonaites, with the exception of Pontlyfni, where REE concentrations vary by a factor of ~5. Variations among the different winonaites

Table 2a. Minor and trace element concentrations (averages and ranges, in ppm except where noted) in winonaite plagioclase.

	NWA 1463 n = 2	Pontlyfni n = 6	Winona n = 3	Mt. Morris n = 3	Tierra Blanca n = 3	HaH 193[a] n = 3
Na (%)	8.5 (8.4–8.7)	8.3 (7.6–8.8)	8.3 (8.0–8.8)	8.1 (7.7–8.5)	4.7 (2.5–8.1)	7.1 (7.0–7.1)
P	43 (32–53)	54 (20–100)	56 (15–125)	17 (11–23)	61 (35–101)	7.3 (6.9–8.1)
K (%)	0.85 (0.80–0.89)	0.51 (0.40–0.75)	0.45 (0.43–0.46)	0.40 (0.34–0.44)	0.45 (0.44–0.46)	0.30 (0.28–0.30)
Ca (%)	2.1 (2.1–2.2)	1.7 (0.92–2.7)	3.0 (2.9–3.1)	3.8 (3.6–4.0)	2.4 (2.2–2.6)	3.3 (3.1–3.4)
Sc	1.7 (1.7–1.8)	0.94 (0.58–1.3)	1.9 (1.8–2.0)	2.1 (2.0–2.4)	2.2 (1.9–2.4)	1.5 (1.4–1.7)
Ti	250 (225–275)	14 (3.4–36)	310 (290–350)	135 (125–150)	238 (235–240)	145 (130–165)
V	n.m.	n.m.	n.m.	n.m.	n.m.	n.m.
Mn	n.m.	n.m.	n.m.	n.m.	n.m.	n.m.
Fe (%)	0.79 (0.73–0.84)	0.42 (0.16–0.75)	0.13 (0.10–0.17)	0.47	0.23 (0.14–0.32)	0.13 (0.12–0.14)
Sr	84 (80–87)	115 (77–155)	99 (97–100)	83 (74–92)	98 (90–105)	91 (88–94)
Y	0.059 (0.035–0.084)	0.045 (0.010–0.085)	0.085 (0.059–0.12)	0.072	0.039 (0.037–0.040)	0.064 (0.057–0.069)
Zr	0.23 (0.22–0.23)	0.14 (0.050–0.23)	0.36 (0.35–0.36)	0.18	0.15 (0.11–0.20)	0.22 (0.19–0.24)
Ba	25 (24–26)	32 (23–39)	25 (23–28)	15	26 (23–30)	14 (13–15)
La	1.7 (1.6–1.8)	1.0 (0.49–2.2)	1.6 (1.3–1.8)	1.4 (1.0–1.9)	1.3 (0.73–1.8)	0.71 (0.56–0.80)
Ce	1.8 (1.6–2.0)	0.84 (0.28–1.7)	1.5 (1.3–1.9)	1.8 (1.3–2.2)	1.3 (0.66–2.0)	1.0 (0.75–1.3)
Pr	0.11 (0.096–0.12)	0.047 (0.016–0.075)	0.086 (0.067–0.11)	0.13 (0.10–0.19)	0.088 (0.048–0.14)	0.072 (0.055–0.090)
Nd	0.27 (0.24–0.30)	0.14 (0.041–0.20)	0.21 (0.15–0.28)	0.23 (0.21–0.25)	0.21 (0.11–0.32)	0.19 (0.15–0.23)
Sm	b.d.	0.016 (0.015–0.017)	0.016 (b.d.–0.016)	0.019 (b.d.–0.019)	0.020 (b.d.–0.020)	0.025 (0.018–0.032)
Eu	0.76 (0.74–0.78)	1.3 (0.85–1.8)	0.81 (0.76–0.85)	0.55 (0.49–0.63)	0.91 (0.83–0.96)	0.40 (0.30–0.49)
Gd	0.021 (0.010–0.031)	0.006 (b.d.–0.006)	0.013 (b.d.–0.013)	0.024 (0.016–0.029)	0.012 (0.007–0.017)	0.015 (0.010–0.023)
Tb	b.d.	b.d.		b.d.	b.d.	b.d.
Dy	b.d.	b.d.		b.d.	b.d.	b.d.
Ho	b.d.	b.d.		b.d.	b.d.	b.d.
Er	b.d.	b.d.		b.d.	b.d.	b.d.
Tm	b.d.	b.d.		b.d.	b.d.	b.d.
Yb	b.d.	b.d.		b.d.	b.d.	b.d.
Lu	b.d.	b.d.		b.d.	b.d.	b.d.

[a]Includes data from Floss et al. (2007); n.m. = not measured; b.d. = below detection.

Table 2b. Minor and trace element concentrations (averages and ranges, in ppm except where noted) in winonaite clinopyroxene.

	NWA 1463 n = 10	Pontlyfni n = 11	Winona n = 7	Mt. Morris n = 8	Tierra Blanca n = 4	HaH 193[a] n = 5
Na (%)	0.48 (0.42–0.71)	0.16 (0.12–0.24)	0.41 (0.38–0.42)	0.27 (0.24–0.37)	0.66 (0.51–1.1)	0.27 (0.24–0.29)
P	37 (21–59)	25 (16–43)	29 (9.7–67)	11 (6.7–17)	60 (35–94)	16 (7.9–32)
K	12 (3.5–32)	30 (10–49)	97 (42–215)	8.7 (4.4–21)	36 (8.6–62)	24 (5.6–42)
Ca (%)	12.1 (11.5–12.4)	12.1 (11.8–12.3)	11.9 (11.7–12.2)	12.1 (12.0–12.3)	12.0 (11.4–12.5)	11.9 (11.4–12.2)
Sc	77 (72–80)	66 (60–76)	96 (89–100)	79 (66–90)	84 (78–89)	72 (70–75)
Ti	2500 (2440–2570)	830 (100–2870)	3735 (3345–4345)	2330 (1700–3290)	2385 (2270–2635)	3370 (2885–3660)
V	295 (280–305)	53 (2.7–170)	189 (135–215)	88 (51–105)	355 (335–385)	51 (47–56)
Mn	2115 (2070–2170)	105 (49–240)	1520 (1445–1750)	905 (875–930)	2590 (2405–2680)	955 (855–1100)
Fe (%)	1.6 (1.4–2.3)	0.17 (0.12–0.33)	1.0 (0.99–1.0)	0.83 (0.63–1.9)	1.8 (1.6–1.9)	0.67 (0.41–1.0)
Sr	4.6 (3.5–7.7)	6.8 (5.4–8.3)	5.6 (4.2–7.7)	4.7 (3.6–7.2)	6.7 (5.7–7.6)	5.9 (4.5–10)
Y	24 (24–25)	22 (20–26)	37 (33–40)	30 (27–36)	17 (15–17)	28 (27–31)
Zr	80 (77–85)	31 (8.8–76)	170 (135–180)	80 (71–90)	21 (14–30)	83 (68–98)
Ba	0.091 (0.050–0.22)	0.18 (0.052–0.44)	0.37 (0.19–0.73)	0.32 (0.075–0.96)	0.21 (0.10–0.30)	0.043 (0.026–0.067)
La	2.5 (2.2–2.7)	4.4 (1.3–7.9)	2.5 (2.3–2.7)	1.5 (1.2–2.1)	2.0 (1.3–3.0)	1.5 (1.1–2.2)
Ce	10 (9.7–11)	12 (4.2–19)	10 (9.2–12)	6.0 (4.6–8.9)	7.4 (5.1–11)	5.4 (4.5–6.0)
Pr	1.7 (1.5–2.1)	1.9 (0.83–2.9)	1.9 (1.5–2.2)	1.2 (1.1–1.4)	1.4 (0.98–2.0)	1.0 (0.98–1.2)
Nd	9.1 (8.2–10)	8.8 (4.8–12)	10 (8.4–13)	6.4 (5.5–7.8)	6.9 (5.5–8.7)	5.4 (4.8–6.4)
Sm	2.9 (2.4–3.3)	2.8 (2.2–3.4)	3.5 (2.9–4.5)	2.6 (2.0–3.2)	2.3 (2.1–2.5)	1.9 (1.7–2.0)
Eu	0.041 (0.017–0.061)	0.090 (0.040–0.18)	0.028 (0.015–0.053)	0.029 (0.001–0.045)	0.084 (0.068–0.11)	0.009 (b.d.–0.016)
Gd	4.1 (3.6–4.7)	3.8 (3.2–4.4)	4.9 (3.9–6.0)	4.3 (3.5–5.0)	2.8 (2.1–3.1)	2.5 (2.3–2.8)
Tb	0.73 (0.58–0.95)	0.64 (0.50–0.86)	0.83 (0.64–1.0)	0.78 (0.61–0.90)	0.48 (0.41–0.57)	0.44 (0.35–0.51)
Dy	4.4 (4.0–4.8)	4.4 (3.6–5.3)	5.8 (5.1–6.8)	5.0 (4.8–5.2)	3.2 (2.6–3.7)	2.5 (2.0–2.6)
Ho	0.89 (0.78–1.0)	0.83 (0.72–0.94)	1.1 (0.95–1.2)	1.0 (0.87–1.4)	0.75 (0.56–0.85)	0.44 (0.39–0.49)
Er	2.4 (2.1–2.7)	2.5 (2.2–3.0)	3.1 (2.8–3.6)	3.1 (2.8–3.7)	2.0 (1.5–2.2)	1.1 (0.99–1.3)
Tm	0.29 (0.26–0.33)	0.33 (0.26–0.51)	0.38 (0.34–0.42)	0.37 (0.33–0.43)	0.31 (0.22–0.38)	0.14 (0.11–0.18)
Yb	1.8 (1.3–2.3)	2.0 (1.7–2.6)	2.3 (2.2–2.5)	2.1 (1.7–2.5)	1.8 (1.2–2.2)	0.77 (0.59–1.0)
Lu	0.27 (0.18–0.36)	0.31 (0.24–0.39)	0.30 (0.24–0.36)	0.33 (0.26–0.39)	0.24 (0.17–0.28)	0.089 (0.072–0.11)

[a]Includes data from Floss et al. (2007); n.m. = not measured; b.d. = below detection.

Table 2c. Minor and trace element concentrations (averages and ranges, in ppm except where noted) in winonaite orthopyroxene.

	NWA 1463 n = 10	Pontlyfni n = 11	Winona n = 8	Mt. Morris n = 11	Tierra Blanca n = 9	HaH 193[a] n = 5
Na	185 (140–240)	57 (14–140)	255 (230–305)	190 (130–250)	360 (290–435)	220 (160–320)
P	23 (9.7–58)	28 (7.2–94)	13 (9.7–18)	17 (7.4–55)	18 (14–29)	6.8 (5.8–8.4)
K	3.4 (0.88–9.5)	11 (4.0–32)	20 (7.2–55)	6.9 (1.1–16)	27 (5.4–59)	1.9 (1.0–2.9)
Ca (%)	0.43 (0.37–0.48)	0.38 (0.35–0.46)	0.50 (0.45–0.52)	0.38 (0.35–0.44)	0.54 (0.51–0.59)	0.46 (0.45–0.48)
Sc	5.2 (4.1–6.0)	5.9 (2.6–8.5)	8.4 (7.7–9.6)	7.1 (6.3–8.4)	8.4 (7.6–9.1)	7.6 (6.7–8.6)
Ti	705 (480–795)	195 (60–375)	1000 (945–1095)	500 (440–580)	865 (810–930)	550 (445–615)
V	49 (40–54)	4.7 (2.6–7.6)	39 (34–43)	34 (29–41)	57 (52–63)	19 (15–23)
Mn	3755 (3565–4115)	135 (72–390)	2420 (2285–2530)	1555 (1515–1615)	3110 (2950–3275)	1450 (1170–1850)
Fe (%)	2.6 (2.4–2.8)	0.26 (0.09–0.62)	2.2 (2.0–2.8)	1.2 (1.1–1.3)	2.2 (2.1–2.9)	1.4 (1.2–1.6)
Sr	0.025 (0.009–0.042)	0.064 (0.023–0.14)	0.10 (0.084–0.12)	0.20 (0.079–0.40)	0.10 (0.063–0.16)	0.057 (0.026–0.097)
Y	0.70 (0.40–1.1)	1.1 (0.47–1.5)	1.4 (1.0–1.5)	1.1 (0.87–1.2)	0.87 (0.78–1.0)	1.4 (1.2–1.5)
Zr	0.74 (0.54–1.1)	0.46 (0.11–1.3)	2.8 (2.4–3.5)	0.79 (0.45–1.0)	0.92 (0.77–1.1)	0.96 (0.70–1.1)
Ba	b.d.	b.d.	b.d.	b.d.	b.d.	b.d.
La	b.d.	b.d.	b.d.	b.d.	b.d.	b.d.
Ce	b.d.	b.d.	b.d.	b.d.	b.d.	b.d.
Pr	b.d.	b.d.	b.d.	b.d.	b.d.	b.d.
Nd	0.012 (b.d.–0.014)	0.035 (0.025–0.053)	0.023 (0.014–0.029)	0.011 (0.007–0.017)	0.025 (0.017–0.031)	0.019 (0.013–0.028)
Sm	0.006 (b.d.–0.007)	0.022 (0.016–0.030)	0.018 (0.012–0.023)	0.007 (b.d.–0.007)	0.015 (0.012–0.017)	0.014 (0.012–0.017)
Eu	0.0005 (b.d.–0.0008)	0.001 (b.d.–0.003)	0.001 (b.d.–0.002)	0.0005 (b.d.–0.001)	b.d.	0.0006 (b.d.–0.0007)
Gd	0.021 (b.d.–0.039)	0.053 (0.032–0.077)	0.040 (0.025–0.063)	0.027 (0.014–0.046)	0.035 (0.026–0.041)	0.028 (0.017–0.034)
Tb	0.009 (0.004–0.014)	0.015 (0.013–0.016)	0.015 (0.011–0.019)	0.008 (0.005–0.013)	0.010 (0.009–0.011)	0.007 (0.004–0.009)
Dy	0.087 (0.046–0.12)	0.15 (0.11–0.19)	0.15 (0.11–0.17)	0.11 (0.094–0.15)	0.10 (0.083–0.12)	0.054 (0.034–0.065)
Ho	0.026 (0.018–0.046)	0.045 (0.030–0.062)	0.046 (0.031–0.051)	0.035 (0.026–0.042)	0.033 (0.025–0.042)	0.013 (0.012–0.014)
Er	0.11 (0.072–0.14)	0.18 (0.12–0.25)	0.19 (0.14–0.23)	0.15 (0.10–0.18)	0.14 (0.13–0.14)	0.055 (0.032–0.067)
Tm	0.020 (0.011–0.031)	0.034 (0.023–0.046)	0.035 (0.026–0.043)	0.027 (0.018–0.037)	0.029 (0.025–0.036)	0.008 (0.006–0.010)
Yb	0.14 (0.091–0.17)	0.27 (0.19–0.34)	0.26 (0.21–0.30)	0.21 (0.17–0.27)	0.21 (0.19–0.23)	0.058 (0.043–0.067)
Lu	0.030 (0.017–0.046)	0.052 (0.040–0.070)	0.049 (0.041–0.057)	0.044 (0.035–0.053)	0.043 (0.035–0.050)	0.010 (0.007–0.012)

[a]Includes data from Floss et al. (2007); n.m. = not measured; b.d. = below detection.

Table 2d. Minor and trace element concentrations (averages and ranges, in ppm except where noted) in winonaite olivine.

	NWA 1463 n = 10	Pontlyfni n = 13	Winona n = 11	Mt. Morris n = 11	Tierra Blanca n = 22	HaH 193[a] n = 14
Na	15 (7.9–25)	40 (11–100)	35 (24–47)	15 (3.6–53)	41 (16–74)	165 (15–475)
P	23 (13–59)	83 (18–220)	20 (7.6–43)	38 (4.2–135)	75 (32–255)	40 (4.3–105)
K	8.8 (2.2–19)	22 (7.1–50)	34 (22–47)	7.1 (1.6–22)	27 (7.3–79)	13 (6.6–26)
Ca	100 (48–225)	92 (27–290)	45 (23–66)	125 (32–310)	190 (88–340)	100 (36–240)
Sc	1.7 (1.1–3.6)	1.5 (1.0–2.3)	2.0 (1.5–3.6)	1.9 (1.5–2.1)	1.6 (0.72–3.0)	2.0 (1.2–2.5)
Ti	19 (16–24)	19 (12–23)	27 (17–37)	13 (11–16)	23 (17–31)	17 (11–22)
V	17 (15–20)	9.0 (8.5–9.5)	14 (12–16)	15 (12–18)	16 (8.7–21)	14 (8.8–18)
Mn	2870 (2745–3100)	785 (315–995)	1935 (1835–2140)	1205 (1145–1330)	2820 (1925–3510)	1675 (1260–1925)
Fe (%)	2.6 (2.3–2.9)	0.30 (0.24–0.43)	2.1 (1.9–2.3)	1.4 (1.2–1.5)	1.2 (0.26–2.8)	2.3 (1.9–3.5)
Sr	0.058 (0.013–0.1)	0.10 (0.041–0.21)	0.22 (0.14–0.27)	0.13 (0.059–0.22)	0.070 (0.028–0.15)	0.095 (0.025–0.34)
Y	0.007 (0.001–0.015)	0.026 (0.013–0.041)	0.012 (0.008–0.020)	0.016 (0.008–0.031)	0.022 (0.011–0.078)	0.007 (0.001–0.021)
Zr	0.15 (0.037–0.41)	0.079 (0.032–0.22)	0.23 (0.13–0.40)	0.11 (0.073–0.22)	0.12 (0.030–0.41)	0.19 (0.043–0.33)

[a]Includes data from Floss et al. (2007).

Table 3. Rare earth element concentrations (averages and ranges, in ppm) in winonaite phosphate.

	NWA 1463	Winona	Mt. Morris		HaH 193[a]	
	merrillite	apatite	apatite	apatite	apatite	apatite
	n = 5	n = 7	n = 1	n = 1	n = 1	n = 2
La	27 (25–29)	18 (8.4–34)	4.9	13	7.1	18 (17–19)
Ce	52 (46–57)	32 (18–60)	16	29	20	49 (48–50)
Pr	5.5 (5.1–5.9)	3.5 (2.1–6.1)	1.8	2.7	2.9	6.2 (5.9–6.5)
Nd	25 (22–26)	16 (9.7–29)	11	11	17	31 (30–33)
Sm	8.2 (6.4–9.7)	5.6 (2.8–8.6)	5.3	4.4	6.2	10 (9.8–11)
Eu	1.4 (1.3–1.4)	1.5 (1.2–1.8)	0.67	0.67	0.69	0.97 (0.82–1.1)
Gd	10 (8.2–12)	7.7 (3.6–13)	6.9	6.1	8.0	14 (13–14)
Tb	2.3 (1.9–2.9)	1.8 (0.86–2.9)	1.7	1.7	1.7	3.1 (3.0–3.1)
Dy	17 (11–25)	14 (8.1–23)	11	13	9.7	19 (18–21)
Ho	3.9 (2.5–5.0)	3.6 (1.8–5.6)	2.9	3.9	2.4	4.4 (3.9–4.9)
Er	13 (9.3–19)	11 (6.7–18)	8.8	13	5.5	14 (13–15)
Tm	2.0 (0.94–3.2)	1.9 (1.2–2.7)	1.4	2.5	0.70	2.1 (1.7–2.6)
Yb	15 (10–19)	13 (9.8–18)	11	17	5.2	16 (13–19)
Lu	1.6 (0.94–2.4)	1.8 (1.4–2.3)	1.6	2.7	0.59	2.1 (2.0–2.1)

[a]Includes data from Floss et al. (2007).

studied are also limited, and both the REE patterns and abundances of winonaite plagioclase are similar to the ranges observed in the acapulcoites and lodranites (Floss 2000).

Abundances of other trace and minor elements in plagioclase are also largely homogeneous, again with the notable exception of Pontlyfni, which for many elements shows variations as large as (or larger than) those seen in all the other winonaites together (Table 2a). While abundances of most trace elements exhibit ranges that overlap to some extent among the different meteorites, the abundances of Sc and, particularly, Ti in Pontlyfni plagioclase are distinctly lower than those in plagioclase from other winonaites.

Clinopyroxene

REE patterns for clinopyroxene are bow-shaped with large negative Eu anomalies and trivalent REE abundances on the order of 10 × CI (Fig. 3b). As for plagioclase, REE abundances in clinopyroxene within a given sample are uniform, except for Pontlyfni, which shows trivalent REE concentrations that, again, vary by a factor of ~5 (Table 2b). Variations among the different winonaites are limited for the trivalent REE, with the exception of HaH 193, which has a REE pattern that is more HREE-depleted than that of the other meteorites; average Eu abundances also differ considerably, with an order of magnitude difference between HaH 193 and Tierra Blanca (Fig. 3b). REE patterns are similar to those of the acapulcoites and lodranites, but abundances fall at the high end of the range observed for these meteorites (Floss 2000).

Most other trace elements in clinopyroxene exhibit limited variability within a given winonaite, but some elements show large variations, including P and K in most samples, and Ti, V, Mn and Zr in Pontlyfni. Trace element abundances tend to cluster into distinct groups among the different meteorites, with total winonaite ranges that span up to two orders of magnitude for elements such as Ti, V and Mn (Table 2b).

Orthopyroxene

Orthopyroxene in the winonaites has HREE-enriched patterns with negative Eu anomalies and abundances up to about 1 × CI (Fig. 3c). Lanthanum, Ce, and Pr abundances are below detection limits in all of the samples (Table 2c). Variations within a given meteorite (including Pontlyfni) are generally less than a factor of 2 and the overall variation is similarly limited. However, HREE abundances in HaH 193 orthopyroxene are lower than those of the other winonaites. Chondrite-normalized REE patterns and absolute abundances are similar to those seen in the acapulcoites and lodranites (Floss 2000).

Variations in other trace elements in orthopyroxene largely mirror those observed in clinopyroxene. Many elements are relatively uniform in abundance, but there are exceptions, including P and K in most samples, and elements such as Ti, Mn, and Zr in Pontlyfni; Fe concentrations in Pontlyfni orthopyroxene are also more variable than in the other samples.

Olivine

Measurements of several olivine grains from Tierra Blanca and HaH 193 showed that all REE had concentrations below detection limits; thus, the REE were not measured in any additional olivines from the winonaites. The variability of trace element abundances within a given winonaite is greater for olivine than for the other minerals analyzed. Whereas the ranges for Sc, Ti, V, and Mn are relatively restricted, other elements, including Na, P, and Ca, exhibit

order of magnitude variations within individual samples. In Winona, Tierra Blanca, and HaH 193 we analyzed olivine grains from both the coarse-grained regions described above and the more fine-grained matrix areas. These results are discussed in detail below.

Phosphate

Merrillite is present in NWA 1463, whereas the Ca-phosphate present in the other winonaites is apatite (Table 3). Figure 4 shows the range of REE patterns observed in each meteorite. Merrillite grains from NWA 1463 have approximately flat patterns with negative Eu anomalies; LREE abundances are uniform, but there is some variation in the HREE abundances. REE concentrations are lower than in acapulcoite merrillites and overlap those of lodranite merrillites (Fig. 4a). However, the HREE enrichment seen in lodranite merrillite grains is not observed in merrillite from NWA 1463.

Two apatite grains were measured in Mount Morris (Table 3). Both have HREE-enriched patterns with negative Eu anomalies (Fig. 4b); LREE abundances are similar to those seen in lodranite apatites, but HREE concentrations are higher. Winona apatite exhibits a range of REE patterns from flat with negative Eu anomalies to HREE-enriched with slight positive Eu anomalies (Fig. 4c); abundances fall within the ranges observed for acapulcoites and lodranites. REE patterns in apatite from HaH 193 are flat with negative Eu anomalies (Fig. 4d); two grains have similar REE concentrations while the third has somewhat lower REE abundances (Table 3).

Whole Rock REE Patterns

We can use the mineral REE compositions (Tables 2 and 3) and the meteorite modal abundances (Table 1) to reconstruct the bulk REE compositions of the meteorites studied here. The REE patterns calculated in this manner are shown in Fig. 5. As noted earlier, the whole rock REE data obtained to date on the winonaites have shown considerable variability, both between and within individual meteorites. For example, Prinz et al. (1980) found that different splits of Winona exhibited strikingly different REE patterns, ranging from nearly flat with a negative Eu anomaly to V-shaped with a positive Eu anomaly. Mount Morris, Tierra Blanca, and Y-75300 also exhibit V-shaped REE patterns with positive Eu anomalies (Prinz et al. 1980; Yamamoto et al. 1991; Kallemeyn 1997), whereas a REE pattern for Pontlyfni is LREE-enriched with a positive Eu anomaly (Davis et al. 1977).

The whole rock REE patterns calculated here from the mineral compositions and modal abundances also exhibit a variety of patterns and abundances (Fig. 5). Four of the winonaites (Pontlyfni, Winona, Tierra Blanca, and HaH 193) have flat to HREE-enriched patterns with positive Eu anomalies; the pattern for Winona is, in addition, significantly enriched in the LREE (i.e., a V-shaped pattern). Abundances

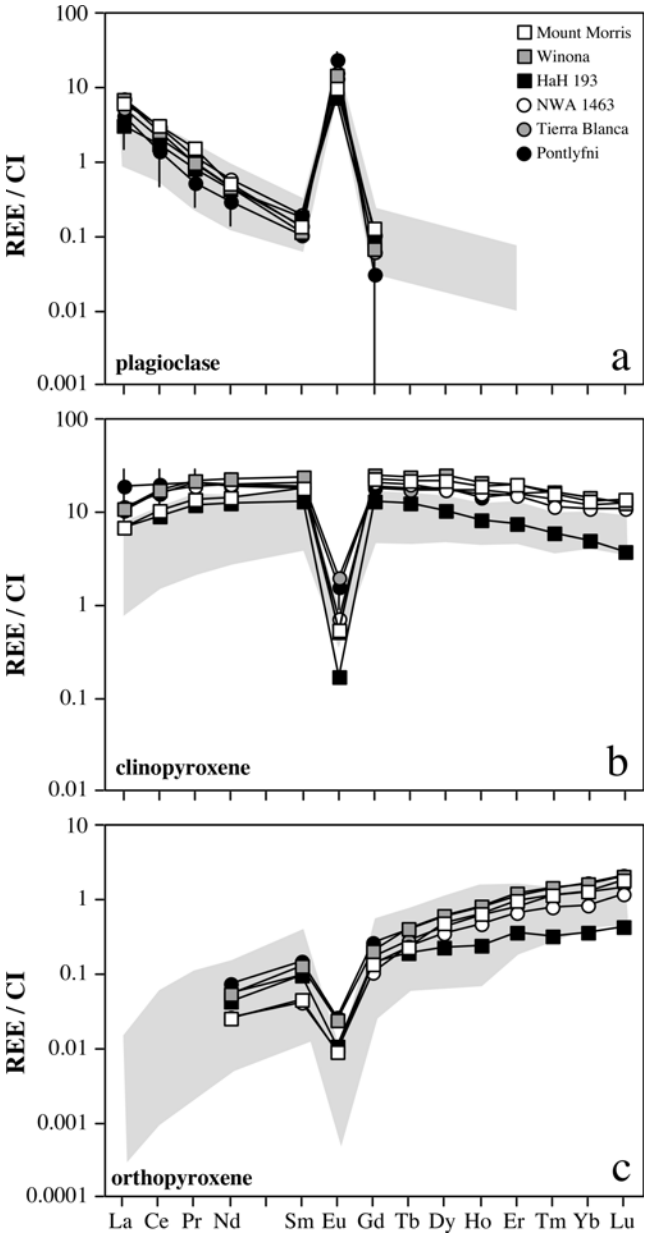

Fig. 3. Average CI chondrite-normalized REE patterns for a) plagioclase, b) clinopyroxene and c) orthopyroxene in winonaites. Error bars (1 σ) are shown only for plagioclase and clinopyroxene from Pontlyfni as these minerals showed a wider range of compositions than most of the other samples (Table 2). The light gray shaded areas show the ranges for acapulcoites and lodranites (data from Floss 2000).

range from ~0.5–2 × CI, except for Eu in Pontlyfni which has an abundance of 3 × CI. Mount Morris has a HREE-enriched pattern as well, with abundances ranging from 0.5 to 1.3 × CI, but does not exhibit a Eu anomaly. The REE pattern for NWA 1463 is flat at ~2 × CI with a negative Eu anomaly.

There are several possible explanations for the variable bulk REE patterns that we observe in the winonaites. One possibility, that we have not sampled all the major REE

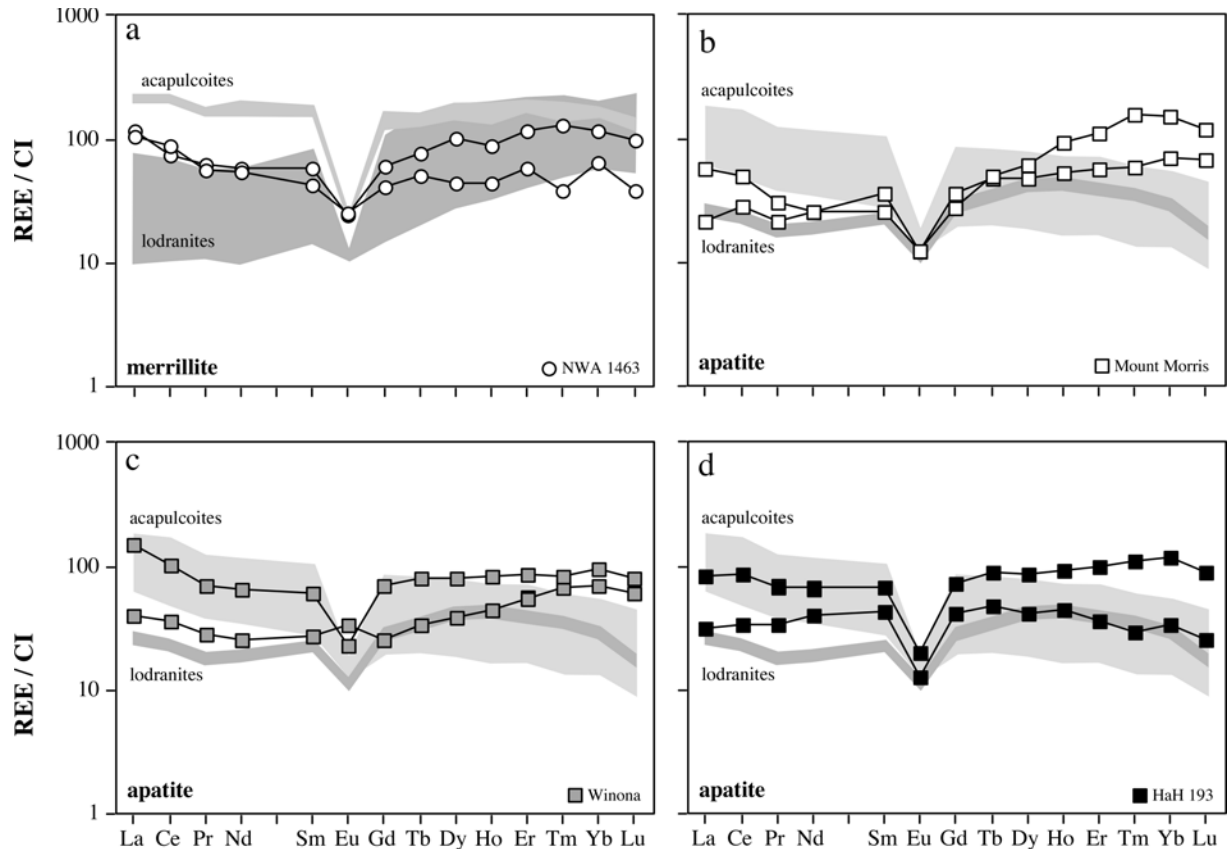

Fig. 4. CI chondrite-normalized REE patterns for merrillite and apatite in winonaites: a) NWA 1463; b) Mount Morris; c) Winona; and d) Hah 193. The ranges in patterns are shown for each meteorite. The light and dark shaded gray areas show the ranges for acapulcoites and lodranites, respectively (data from Floss 2000).

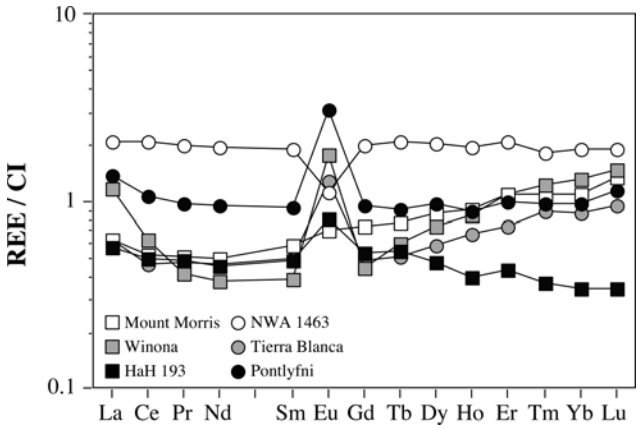

Fig. 5. CI-chondrite normalized whole rock REE patterns for the winonaites. Patterns were calculated using mineral compositions from Tables 2 and 3, and the modal abundances from Table 1. Data for HaH 193 from Floss et al. (2007).

carriers in the winonaites, is not likely. We have analyzed all the major silicate minerals (olivine, pyroxene, plagioclase, and amphibole, when present) in these meteorites, as well as the phosphates in those winonaites in which they are present. Phosphides occur in some of the winonaites (e.g., Pontlyfni), but several analyses show that they do not contain any REE; other opaque minerals present in these meteorites are also not likely REE carriers.

Another possibility for the variable REE patterns is that the modal abundances are not representative of the bulk meteorites. That the winonaites are mineralogically heterogeneous is evident from the fact that different splits of the same meteorite can exhibit significantly different bulk REE patterns (e.g., Winona; Prinz et al. 1980). The fact that our calculated whole rock REE patterns also exhibit significant heterogeneity indicates that these meteorites are heterogeneous on a scale larger than that of a single thin section. This is supported by the fact that a second section of HaH 193 studied by Floss et al. (2007) has olivine and clinopyroxene abundances that are a factor of two higher than those in the section examined here. A bulk REE pattern calculated using the modal abundances of that section differs as well, with abundances that are approximately a factor of two higher and no Eu anomaly (Floss et al. 2007).

These mineralogical heterogeneities clearly indicate real variations that are the result of processes acting on the winonaite parent body. Textural evidence suggests that some partial melting occurred in addition to the extensive thermal

metamorphism. Moreover, the winonaites are brecciated (possibly as the result of impact disruption and reassembly of the parent body; Benedix et al. 2000), resulting in the juxtaposition of different lithologies. It is likely that these factors combined account for the variability in the bulk calculated REE patterns observed here.

DISCUSSION

The winonaites have chondritic mineralogies and are generally fine- to medium-grained with mostly equigranular textures that reflect the extensive thermal metamorphism they have experienced. Benedix et al. (1998) have noted, however, that some of them also contain mm- to cm-sized regions with different textures and/or mineralogies that could be the result of partial melting in certain regions of the parent body. Benedix et al. (2000) argued that the winonaite (and IAB iron) parent body experienced partial melting and differentiation, which was followed by mixing of lithologies through catastrophic impact breakup, and thermal annealing of the reassembled parent body. If the parent body on which these meteorites originated indeed experienced silicate partial melting prior to impact breakup, the trace element data obtained from their individual minerals may provide evidence of this event. For example, we can examine the trace element characteristics of the distinctive lithologies in the winonaites that may be related to silicate partial melting. These include fine-grained areas enriched in plagioclase and clinopyroxene that may represent silicate partial melts, and coarse-grained, olivine-rich regions that have been interpreted as partial melt residues (Benedix et al. 1998). The first silicate partial melts from a chondritic precursor are expected to be enriched incompatible elements, whereas residues left behind after removal of such partial melts will be incompatible-element-depleted.

Another way we can try to evaluate whether silicate partial melting took place on the winonaite parent body is to compare these meteorites with the acapulcoites and lodranites. This group of primitive achondrites is generally considered to have experienced silicate partial melting in parts of their parent body (e.g., McCoy et al. 1996; 1997a, 1997b; but see Rubin 2007 for an alternative viewpoint). Acapulcoites are typically fine-grained with equigranular textures and chondritic mineralogies, and appear to represent a portion of the parent body that has undergone significant thermal metamorphism, but little, if any, silicate melting. The lodranites are more coarse-grained and are depleted in metal and sulfides, as well as plagioclase, indicating they have experienced more extensive heating, resulting in silicate partial melting and the loss of those melts from the lodranite region of the parent body. Comparison of trace element distributions in the acapulcoites and lodranites has shown that minerals from the latter have retained a record of the silicate partial melting they have experienced (Floss 2000).

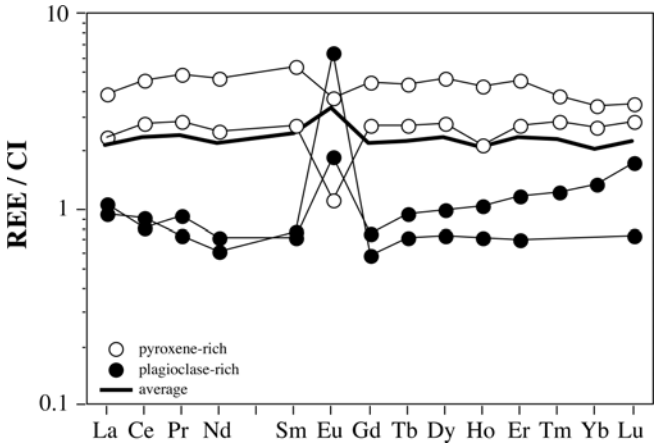

Fig. 6. CI chondrite-normalized REE patterns of fine-grained plagioclase/clinopyroxene-rich areas in Pontlyfni. Open circles designate analyses dominated by pyroxene, filled circles, those dominated by plagioclase; the solid line shows the average of all analyses.

Fine-Grained Plagioclase/Pyroxene-Rich Lithology

Benedix et al. (1998) first noted the presence in Pontlyfni of a fine-grained equigranular lithology dominated by plagioclase and calcic pyroxene, and suggested that this lithology could represent the basaltic partial melt produced by the initial partial melting of a chondritic parent body. The first silicate melts to form from a chondritic body should be plagioclase-rich and are expected to be enriched in incompatible trace elements and the LREE associated with a feldspathic component.

We made 4 measurements in a fine-grained plagioclase/clinopyroxene-rich area of Pontlyfni (Fig. 2a, upper right). The spot size that we used (~25 μm) in the ion microprobe is clearly smaller than a representative area of this lithology; this is reflected in the fact that the REE patterns that we obtain from these areas are quite variable (Fig. 6), and represent different proportions of plagioclase and pyroxene being measured in each analysis. However, the average REE pattern is approximately flat at about 2 × CI and has a small positive Eu anomaly. This is slightly enriched relative to chondrites, and the positive Eu anomaly could indicate the presence of excess plagioclase, although we do not see any enrichment of the LREE that might also be expected due to the abundance of feldspathic components that are among the first phases to melt from a chondritic precursor. While we cannot be certain that the average composition calculated here is, indeed, representative of the bulk lithology, we note that the individual patterns shown in Fig. 6 also do not exhibit any enrichment of the LREE. Thus, there does not seem to be a significant trace element signature in this lithology related to silicate partial melting from a chondritic precursor.

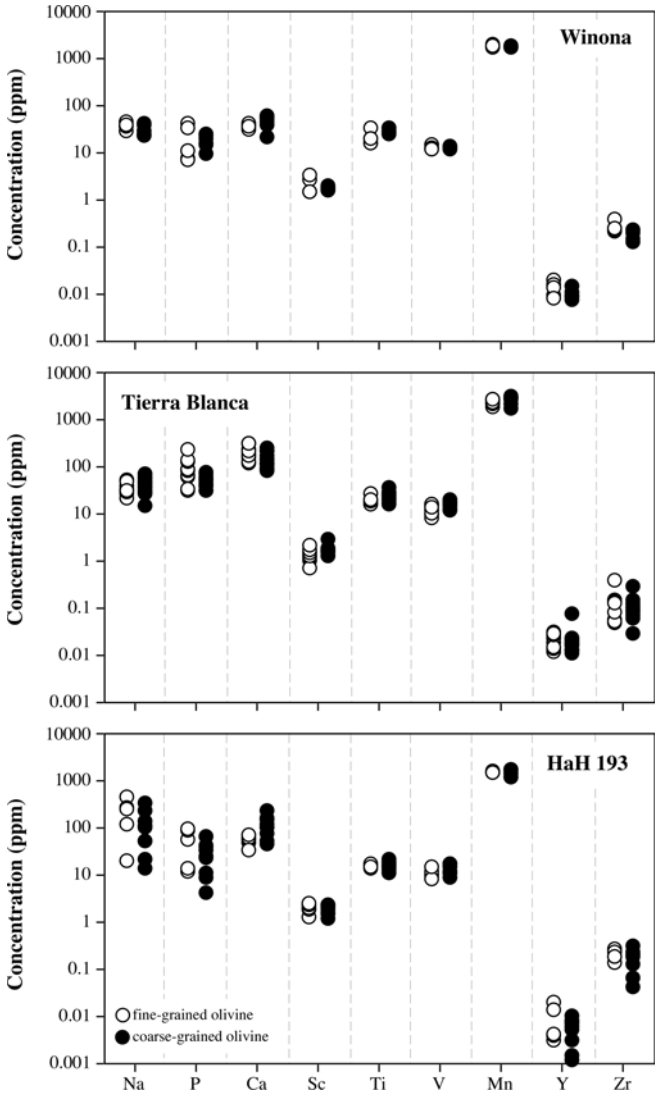

Fig. 7. Trace element concentrations in olivine from coarse-grained lithologies (black circles) and fine-grained matrix areas (white circles) from Winona, Tierra Blanca, and HaH 193.

Coarse-Grained Olivine-Rich Lithology

The second lithology found in winonaites that may be related to silicate partial melting is one that consists of coarse-grained clumps of olivine grains (Fig. 2b). This lithology was initially reported in Winona by Benedix et al. (1998), who argued that it could represent partial melt residues from the winonaite parent body. If this lithology does indeed represent a partial melt residue, we would expect that the coarse olivine grains have lower abundances of incompatible trace elements than the more fine-grained olivine grains present in the matrix of the winonaites, which presumably have not experienced silicate partial melting. We have measured trace element abundances in both coarse- and fine-grained olivines from the three winonaites in which we find both types of olivine, Winona, Tierra Blanca and HaH 193. Figure 7 shows the results. In all 3 meteorites, all of the trace elements measured have very similar abundance ranges for both coarse-grained and fine-grained olivine, including incompatible elements such as Ca, Ti, Y, and Zr. Therefore, the coarse-grained olivine lithology also does not provide any compelling trace element evidence for partial silicate melting on the winonaite parent body.

Phosphate REE Patterns

As noted above, some of the minerals in the acapulcoites and lodranites have recorded evidence of the silicate partial melting that took place on their parent body (Floss 2000). Phosphate REE abundances are variable in the acapulcoites and lodranites, and are not reliable indicators of partial melting processes. However, the shape of the REE patterns does appear to be diagnostic: lodranite phosphates are characterized by significant LREE depletions relative to acapulcoite phosphates, consistent with the removal of a LREE-rich component in a plagioclase-rich partial melt (Floss 2000).

Phosphates from the winonaites also exhibit a variety of REE abundances and chondrite-normalized patterns (Fig. 4). Most of the patterns are approximately flat or LREE-enriched, like phosphates from the acapulcoites. Several of them however, notably some of those from Winona and Mount Morris, are enriched in the HREE relative to the LREE (Figs. 4b and 4c), resembling the REE patterns of lodranite phosphates. Although this may simply reflect initial heterogeneity, it is possible that some phosphates from the winonaites may have originated in a region of the parent body that was affected by silicate partial melting.

Trace Element Trends in Pyroxene and Plagioclase

As noted above, the acapulcoites and lodranites have retained a record of silicate partial melting experienced on their parent body through systematic differences in the incompatible trace element abundances of their pyroxenes. Both clinopyroxene and orthopyroxene in the lodranites have depleted abundances of the incompatible elements Ti, Zr, and Y compared to the abundances of these elements in the acapulcoite pyroxenes (cf. Figs. 3 and 4 of Floss 2000). These differences are consistent with the formation and removal of an incompatible-element-rich silicate partial melt from the lodranite region of the parent body, leaving behind mineral phases depleted in incompatible trace elements. We can examine the winonaite pyroxenes to see if they exhibit any similar evidence of silicate partial melting.

Figure 8 shows the abundances of Zr and Y versus Ti in clinopyroxene and orthopyroxene from the winonaites. The incompatible trace element relationships are clearly not as simple as those observed in the acapulcoites and lodranites.

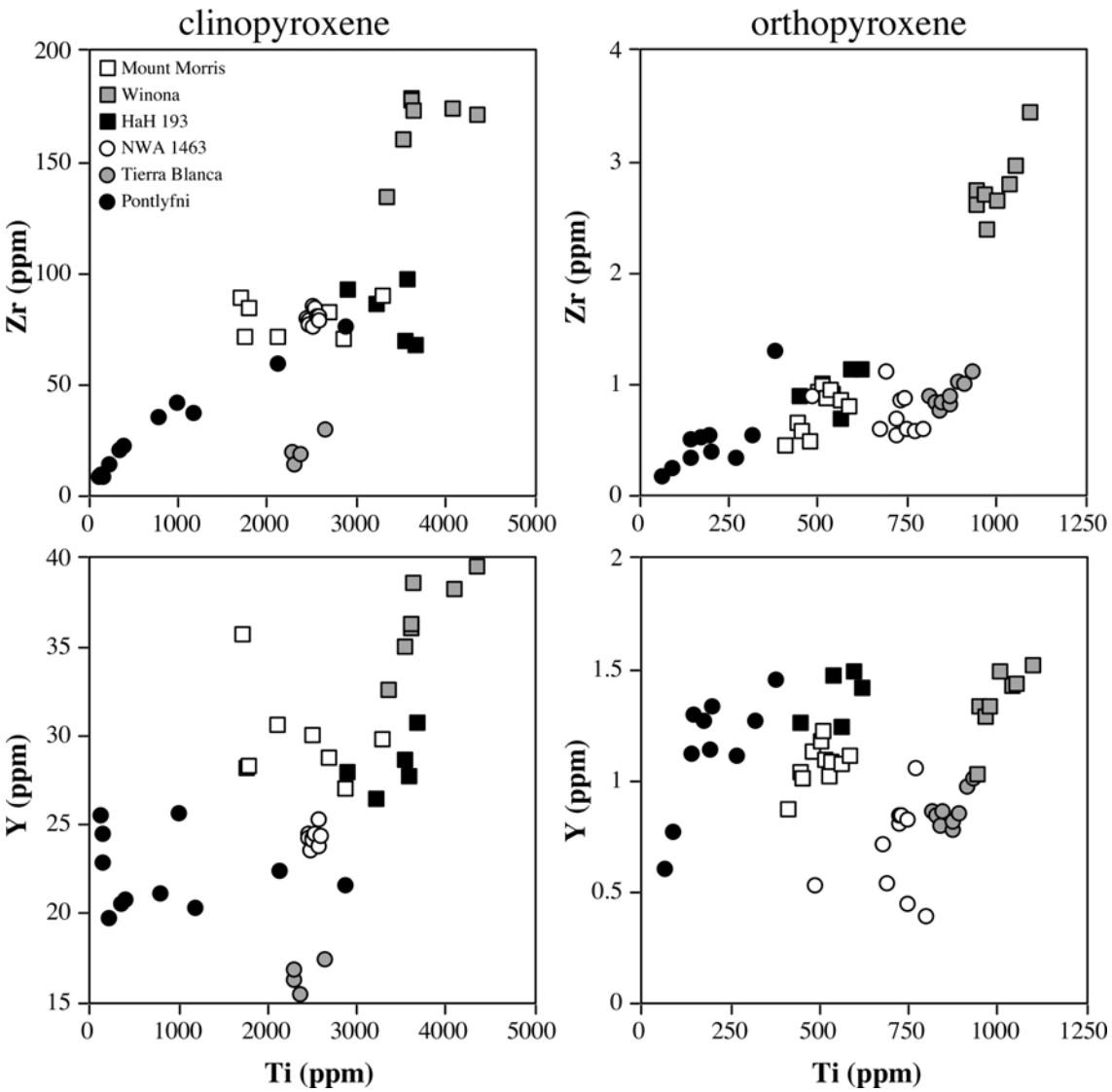

Fig. 8. Concentrations (in ppm) of Zr and Y versus Ti in clinopyroxene and orthopyroxene from the winonaites. Note different scales on the axes.

However, some systematic trends do appear to be present. For both types of pyroxene, the abundances of these elements tend to be highest in Winona and lowest in Pontlyfni, whereas the other winonaites generally fall between these extremes (Y abundances in Tierra Blanca clinopyroxene are an exception; Fig. 8). Such trends could be indicative of silicate partial melting from a common precursor, in which case Pontlyfni would represent the depleted residue and Winona the incompatible-element-rich partial melt. NWA 1463, which has intermediate abundances of these elements (Fig. 8), could potentially represent that precursor material, since it is the least metamorphosed of the winonaites.

However, the abundances of other trace elements in the pyroxenes argue against such a scenario. Specifically, we note that elements that are compatible in pyroxene, such as Sc, Mn, and V, show the same trends as the incompatible trace elements (Fig. 9). Scandium abundances are highest in Winona and lowest in Pontlyfni, and the other 4 winonaites have intermediate Sc abundances. Both Mn and V exhibit similar systematic trends from Pontlyfni to Winona, with Mount Morris and HaH 193 falling between these two. However, for these elements, NWA 1463 and Tierra Blanca do not lie along the same trends, as they did for the other elements, but rather seem to have anomalously high abundances of V, and Mn (Fig. 9). Thus, the data for the pyroxenes, particularly the fact that we see the same systematic trends for both compatible and incompatible trace elements indicates that these are not simple silicate partial melting trends.

CONCLUSIONS

Based on the observations noted above, there is only limited trace element evidence for silicate partial melting in

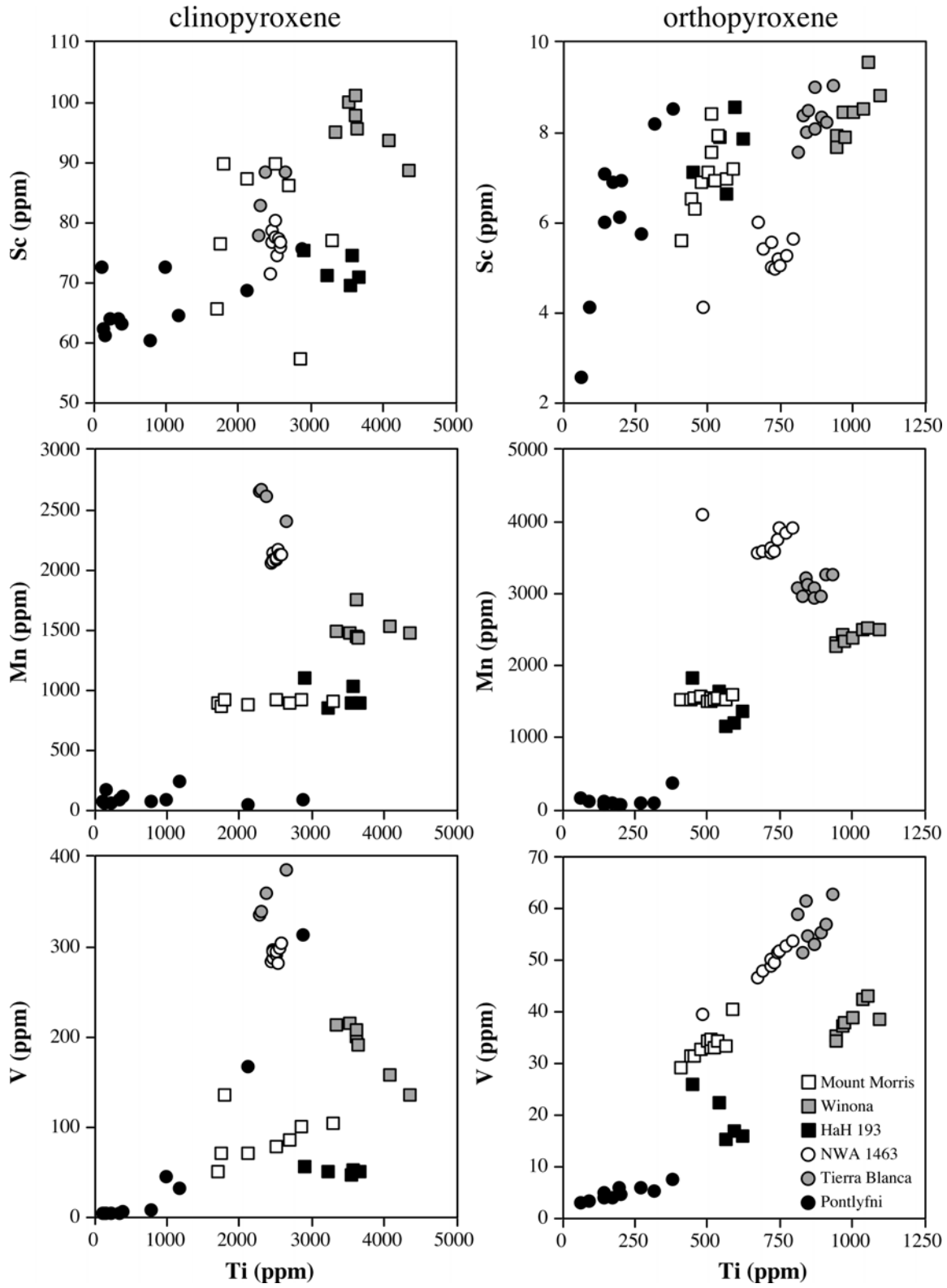

Fig. 9. Concentrations (in ppm) of Sc, Mn, and V versus Ti in clinopyroxene and orthopyroxene from the winonaites. Note different scales on the axes.

the winonaites. Although some phosphate REE patterns are consistent with an origin in a region of the winonaite parent body that could have experienced silicate partial melting, the two lithologies potentially associated with partial melts do not show any clear trace element signatures for such an event. Moreover, the distinct trace element groupings in winonaite pyroxenes suggest equilibration of minerals with initially heterogeneous and distinct compositions, rather than partial melting of a compositionally homogeneous precursor. The larger variations in trace element abundances noted in Pontlyfni (Table 2) are consistent with the lower degree of equilibration inferred for this meteorite from its finer grain size (e.g., Benedix et al. 1998)

The systematic trends observed among the winonaite pyroxenes also seem to be decoupled from the mineralogies of these meteorites. In the lodranites, in which the pyroxenes are depleted in incompatible trace elements, there are also mineralogical indications of silicate partial melting, such as a depletion in plagioclase relative to the acapulcoites (Floss 2000). In contrast, all of the winonaites studied here have approximately chondritic silicate mineral abundances despite their variable incompatible trace element abundances. In particular, there are no obvious depletions or enrichments in bulk plagioclase contents (Table 1).

Despite the lack of trace element evidence, there are mineralogical indications for partial melting in these meteorites. The first partial melt expected to form in a chondritic system is the Fe,Ni-FeS cotectic melt and the presence of veins of Fe,Ni metal and sulfide in several of the winonaites, such as Pontlyfni, Winona, Mt. Morris, and Tierra Blanca, indicates that this did occur on the winonaite parent body. In addition, as we have noted, there is some evidence for the presence of silicate partial melts, most prominently the plagioclase/clinopyroxene-rich lithology in Pontlyfni and the coarse-grained olivine lithologies seen in several winonaites. Because these lithologies do not exhibit trace element signatures consistent with systematic partial melting of a chondritic precursor and because the winonaites have experienced extensive impact brecciation (Benedix et al. 1998), we consider the possibility that they originated through impact-induced shock melting. Impact brecciation clearly took place on the winonaite parent body and resulted in the mixing of lithologies observed in these meteorites. Shock melting could produce the Fe,Ni-FeS veins seen some winonaites (e.g., Wasson and Kallemeyn 2002; Rubin 2007 and references therein) and possibly also plagioclase/clinopyroxene-rich lithologies such as the one seen in Pontlyfni. Moreover, an impact-produced melt may not exhibit strong incompatible trace element enrichments, depending on the local target material and subsequent crystallization conditions. However, it is unlikely that an impact event can account for the extensive melting that would be necessary to obtain an olivine-rich residue from a chondritic precursor. Thus, it seems more likely that silicate partial melting did indeed take place in some portions of the winonaite parent body prior to impact brecciation. The extensive thermal metamorphism experienced by the winonaites may subsequently have led to re-equilibration of trace elements in different lithologies. However, significant compositional heterogeneities must have been retained in the winonaite parent body prior to this equilibration in order to account for the distinct compatible and incompatible element groupings observed in their pyroxenes.

Acknowledgments—We would like to thank Tim Smolar and Eric Inazaki for maintenance of the 3f ion microprobe. We greatly appreciate careful reviews by Tim McCoy and Steve Simon. This work was supported by NASA grants NNG04GG49G and NNX07AI45G to C. F.

Editorial Handling—Dr. Edward Scott

REFERENCES

Alexander C. M. O'D. 1994. Trace element distributions within ordinary chondrite chondrules: Implications for chondrule formation conditions and precursors. *Geochimica et Cosmochimica Acta* 58: 3451–3467.

Anders E. and Grevesse N. 1989. Abundances of the elements: Meteoritic and solar. *Geochimica et Cosmochimica Acta* 53:197–214.

Benedix G., McCoy T. J., Keil K., Bogard D. D., and Garrison D. H. 1998. A petrologic and isotopic study of winonaites: Evidence for early partial melting, brecciation, and metamorphism. *Geochimica et Cosmochimica Acta* 62:2535–2553.

Benedix G. K., McCoy T. J., Keil K., and Love S. G. 2000. A petrologic study of the IAB iron meteorites: Constraints on the formation of the IAB-winonaite parent body. *Meteoritics & Planetary Science* 35:1127–1141.

Benedix G. K., McCoy T. J., and Lauretta D. S. 2003. Is NWA 1463 the most primitive winonaite (abstract)? *Meteoritics & Planetary Science* 38:A70.

Benedix G., Franchi I. A., Greenwood R. C., and Grady M. M. 2006. Effects of alteration on desert meteorites (abstract). *Meteoritics & Planetary Science* 41:A202.

Choi B.-G., Ouyang X., and Wasson J. T. 1995. Classification and origin of IAB and IIICD iron meteorites. *Geochimica et Cosmochimica Acta* 59:593–612.

Clayton R. N. and Mayeda T. K. 1996. Oxygen isotope studies of achondrites. *Geochimica et Cosmochimica Acta* 60:1999–2017.

Davis A. M., Ganapathy R., and Grossman L. 1977. Pontlyfni: A differentiated meteorite related to the group IAB irons. *Earth and Planetary Science Letters* 35:19–24.

De Wit M. J. and Strong D. F. 1975. Eclogite-bearing amphibolites from the Appalachian mobile belt, northwestern Newfoundland: Dry versus wet metamorphism. *Journal of Geology* 83:609–627.

Floss C. 2000. Complexities on the acapulcoite-lodranite parent body: Evidence from trace element distributions in silicate minerals. *Meteoritics & Planetary Science* 35:1073–1085.

Floss C. and Jolliff B. 1998. Rare earth element sensitivity factors in calcic plagioclase (anorthite). In *Secondary ion mass spectrometry, SIMS XI*, edited by Gillen G., Lareau R., Bennett J., and Stevie F. Chichester, U.K.: John Wiley & Sons. pp. 785–788.

Floss C., James O. B., McGee J. J., and Crozaz G. 1998. Lunar

ferroan anorthosite petrogenesis: Clues from trace element distributions in FAN subgroups. *Geochimica et Cosmochimica Acta* 62:1255–1283.

Floss C., Colton S., Reid J., Crozaz G., Jolliff B., and Benedix G. 2003. Winonaite petrogenesis: First results from trace element distributions (abstract). *Meteoritics & Planetary Science* 38: A22.

Floss C., Benedix G., Jolliff B., Crozaz G., and Colton S. 2006. Trace element trends in winonaite pyroxenes: Equilibration of heterogeneous precursors (abstract). *Meteoritics & Planetary Science* 41:A56.

Floss C., Jolliff B., Benedix G., Stadermann F. J., and Reid J. 2007. Hammadah al Hamra 193: The first amphibole-bearing winonaite. *American Mineralogist* 92:460–467.

Hsu W. 1995. Ion microprobe studies of the petrogenesis of enstatite chondrites and eucrites. Ph.D. thesis, Washington University. p. 380.

Kallemeyn G. W. 1997. Compositional relationships among Winona-like and other possibly related meteorites (abstract). 22nd Symposium on Antarctic Meteorites. pp.78–79.

Kallemeyn G. W. and Wasson J. T. 1985. The compositional classification of chondrites: IV. Ungrouped chondritic meteorites and clasts. *Geochimica et Cosmochimica Acta* 49:261–270.

Kimura M., Tsuchiyama A., Fukuoka T., and Imura Y. 1992. Antarctic primitive achondrites, Yamato-74025, 75300, and 75305: Their mineralogy, thermal history, and the relevance to winonaite. *Proceedings of the Fifth NIPR Symposium on Antarctic Meteorites*. pp. 165–190.

King E. A., Jarosewich E., and Daugherty F. W. 1981. Tierra Blanca: An unusual achondrite from West Texas. *Meteoritics* 16:229–237.

Kracher A. 1982. Crystallization of a S-saturated, Fe,Ni-melt, and the origin of the iron meteorite groups IAB and IIICD. *Geophysical Research Letters* 9:412–415.

Kracher A. 1985. The evolution of the partially differentiated planetesimals: Evidence from iron meteorite groups IAB and IICD. *Journal of Geophysical Research* 90:C689–C698.

Kretz R. 1994. *Metamorphic crystallization*. Chichester, U.K.: Wiley and Sons. p. 530.

McCoy T. J., Keil K., Clayton R. N., Mayeda T. K., Bogard D. D., Garrison D. H., Huss G. R., Hutcheon I. D., and Wieler R. 1996. A petrologic, chemical, and isotopic study of Monument Draw and comparison with other acapulcoites: Evidence for formation by incipient partial melting. *Geochimica et Cosmochimica Acta* 60:2681–2708.

McCoy T. J., Keil K., Clayton R. N., Mayeda T. K., Bogard D. D., Garrison D. H., and Wieler R. 1997a. A petrologic and isotopic study of lodranites: Evidence for early formation as partial melt residues from heterogeneous precursors. *Geochimica et Cosmochimica Acta* 61:623–637.

McCoy T. J., Keil K., Muenow D. W., and Wilson L. 1997b. Partial melting and melt migration in the acapulcoite-lodranite parent body. *Geochimica et Cosmochimica Acta* 61: 639–650.

Prinz M., Waggoner D. G., and Hamilton P. J. 1980. Winonaites: A primitive achondritic group related to silicate inclusions in IAB irons (abstract). 11th Lunar and Planetary Science Conference. pp. 902–904.

Rubin A. 2007. Petrogenesis of acapulcoites and lodranites: A shock-melting model. *Geochimica et Cosmochimica Acta* 71: 2383–2401.

Takeda H., Bogard D. D., Mittlefehldt D. W., and Garrison D. H. 2000. Mineralogy, petrology, chemistry, and ^{39}Ar-^{40}Ar and exposure ages of the Caddo County IAB iron: Evidence for early partial melt segregation of a gabbro area rich in plagioclase-diopside. *Geochimica et Cosmochimica Acta* 64:1311–1327.

Wasson J. T. 1970. The chemical classification of iron meteorites–IV. Irons with Ge concentrations greater than 190 ppm and other meteorites associated with group I. *Icarus* 12:407–423.

Wasson J. T. and Kallemeyn G. W. 2002. The IAB iron-meteorite complex: A group, five subgroups, numerous grouplets, closely related, mainly formed by crystal segregation in rapidly cooling melts. *Geochimica et Cosmochimica Acta* 66:2445–2473.

Wasson J. T., Willis J., Wai C. M., and Kracher A. 1980. Origin of iron meteorite groups IAB and IIICD. *Zur Naturforschung* 35a: 781–795.

Yamamoto K., Nakamura N., Misawa K., Yanai K., and Matsumoto Y. 1991. Lithophile trace element abundances in Antarctic unique meteorites and in unique clasts from L6 chondrites (abstract). 15th Symposium on Antarctic Meteorites. pp. 97–98.

Yugami K., Takeda H., Kojima H., and Miyamoto M. 1998. Modal mineral abundances and the differentiation trends in primitive achondrites. *Antarctic Meteorite Research* 11:49–70.

Yugami K., Takeda H., Kojima H., and Miyamoto M. 1999. Comparisons of textural and chemical variations of minerals in some primitive achondrites and an H7 chondrite, with reference to their formation and cooling histories. *Antarctic Meteorite Research* 12:117–138.

Zinner E. and Crozaz G. 1986a. A method for the quantitative measurement of rare earth elements by ion microprobe. *International Journal of Mass Spectrometry and Ion Processes* 69:17–38.

Zinner E. and Crozaz G. 1986b. Ion probe determination of the abundances of all the rare earth elements in single mineral grains. In *Secondary ion mass spectrometry, SIMS V,* edited by Benninghoven A., Colton R. J., Simons D. S., and Werner H. W.: Berlin-Heidelberg-New York: Springer-Verlag. pp. 444–446.